



Exosomal miR-9-5p secreted by bone marrow–derived mesenchymal stem cells alleviates osteoarthritis by inhibiting syndecan-1

Zhe Jin¹ · Jiaan Ren¹ · Shanlun Qi²

Received: 3 April 2019 / Accepted: 20 February 2020 / Published online: 6 May 2020
© Springer-Verlag GmbH Germany, part of Springer Nature 2020

Abstract

Mesenchymal stem cells (MSCs) have been demonstrated to serve as targets for the treatment of osteoarthritis (OA) and exosomes derived from MSCs also display chondroprotective effects. This study aims to investigate the regulatory role of exosomal microRNA-9-5p (miR-9-5p) secreted by bone marrow–derived MSCs (BM-MSCs) on OA in a rat model induced by anterior cruciate ligament/medial collateral ligament transection. Luciferase reporter assay was conducted to verify the putative miR-9-5p binding sites to 3'UTR of syndecan-1 (SDC1). Additionally, an intra-articular injection of miR-9-5p carried by BM-MSC–derived exosomes or liposomes into rats with OA-like damage was performed to ascertain the role of exosomal miR-9-5p and a gain-of-function study of SDC1 was carried out to explore the potential mechanism in relation to SDC1. Subsequently, the expression of SDC1 was determined and the levels of inflammatory factors (IL-1, IL-6, TNF- α and CRP) and oxidative stress injury indicators (NO, MDA, iNOS, COX2 and SOD), the contents of AKP as well as the levels of OA-related factors (MMP-13, COMP and OCN) were measured. Injection of miR-9-5p-contained exosomes resulted in an alleviation of inflammation and OA-like damage, which was evidenced by downregulated levels of inflammatory factors, reduced oxidative stress injury and decreased OCN, MMP-13, COMP and AKP levels. As a target gene of miR-9-5p, the upregulation of SDC1 led to aggravation of inflammation and OA-like damage, which is opposite to exosomal miR-9-5p. To conclude, these findings suggest the anti-inflammatory and chondroprotective effects of BM-MSC–derived exosomal miR-9-5p on OA via regulation of SDC1.

Keywords Osteoarthritis · Bone marrow–derived mesenchymal stem cells · Exosome · microRNA-9-5p · Syndecan-1

Introduction

Osteoarthritis (OA) exhibits a relatively high risk of developing in the aged population as the most common joint disorder throughout the world (Glyn-Jones et al. 2015). OA could cause damage to joint tissues such as articular cartilage, subchondral bone and synovium, which is mainly characterized by degeneration of articular cartilage (Gelber 2014). There still lacks effective interventions to rehabilitate degraded cartilage or retard OA progression due to a limited

understanding of the underlying mechanisms involved in the development and progression of OA (Chen et al. 2017). Complicated interactions between some important genetic and metabolic factors are considered to be of great significance during the progression of OA; the identification of which can aid the development of promising intra-articular therapeutic options (Jones et al. 2019). Besides, mesenchymal stem cells (MSCs) are well-acknowledged as latent therapeutic targets for treatment of regeneration of articular cartilage in OA (Jo et al. 2014) and bone marrow–derived MSCs (BM-MSCs) have been previously suggested as an alternative option for patients with knee OA (Shin et al. 2018).

Targeting extracellular vesicles including exosomes have emerged as a crucial therapeutic strategy, due to their connatural capacity to deliver nucleic acids and other drugs across some chief biological barriers (EL Andaloussi et al. 2013). As membrane vesicles with a diameter of 30–100 nm, exosomes carrying many functional proteins and mRNAs and microRNAs (miRs) are often released from a variety of cell types under particular physiological or pathological

✉ Zhe Jin
15840089041@163.com

¹ Department of Orthopaedics, First Hospital of China Medical University, No. 155, Nanjing North Street, Heping District, Shenyang 110001, Liaoning Province, People's Republic of China

² Department of Orthopaedics, Dashiqiao Central Hospital, Shenyang 115100, People's Republic of China

conditions (Shi et al. 2018). Specifically, human BM-MSC-derived exosomes have the capacity to deliver miRNAs (Wen et al. 2016) and exosomal miRNAs have been shown to act as a modulator of osteoblast differentiation (Xu et al. 2014). Additionally, several miRs are suggested to be aberrantly expressed in OA, including miR-9, miR-34a and miR-140 (Nugent 2016). For example, the expression of miR-9 has been found to be downregulated in knee OA cartilage tissues, which triggers an enhancement in OA chondrocyte proliferation and suppression of apoptosis, which is attributed to the nuclear factor kappa-B1 pathway (Gu et al. 2016). Therefore, we hypothesize that BM-MSC-derived exosomes might be able to deliver miR-9-5p to influence OA progression. However, its downstream molecular mechanism remains elusive. Bioinformatics analysis predicted syndecan-1 (SDC1) as a direct target gene of miR-9-5p. Syndecans consist of four family members (SDC1, SDC2, SDC3, SDC4), which are expressed in cell-, tissue- and development-specific manners (Patterson et al. 2008). During the early stage of cartilage degeneration in OA, the expression of SDC1 was found to be upregulated (Salminen-Mankonen et al. 2005). In this study, we aim to test the hypothesis that BM-MSC-derived exosomal miR-9-5p could influence OA progression in OA rat models and to identify the potential mechanism associated with SDC1.

Materials and methods

Ethics statement

The animal experiments in our study were conducted strictly in accordance with the guidelines of the National Institutes of Health (NIH) for animal care and use, with approval from the Animal Ethics Committee of First Hospital of China Medical University.

Bioinformatics analysis

The OA-related gene expression profile “GSE82107” was retrieved from the Gene Expression Omnibus (GEO) database (<https://www.ncbi.nlm.nih.gov/geo/>), which included 10 microarrays of OA synovial tissues and 7 microarrays of normal synovial tissues from individuals without a joint disease (control). Differentially expressed genes (DEGs) in OA and normal synovial tissues were screened out on the basis of gene expression data obtained from the GEO dataset. The platform used for file annotation was GPL570 [HG-U133_Plus_2] Affymetrix Human Genome U133 Plus 2.0 Array. The Affy package of R language was used for both preprocessing and standardization of the gene expression data (Gautier et al. 2004). The DEGs were identified by a limma package based on the cut-off of $|\log_2(\text{fold change})| > 1$ and

false discovery rate (FDR) < 0.05 (Smyth 2004). The known OA-related genes were retrieved from the searching engine DiGSeE (<http://210.107.182.61/geneSearch/>) and the top 20 genes with the largest fold change were selected as disease genes and used for subsequent analysis. The interaction between screened DEGs and selected disease genes was analyzed on the String database (<https://string-db.org/>) and the gene-gene interaction network was visualized using the Cytoscape 3.6.0 software (Shannon et al. 2003). The candidate miRNAs that can potentially regulate DEGs were predicted through TargetScan (http://www.targetscan.org/vert_71/).

Establishment of OA rat models

Eighty male specific-pathogen-free (SPF) Sprague Dawley rats (aged 6 weeks old; weighing 190 ± 10 g) were purchased from Sun Yat-Sen University of Medical Sciences (Zhongshan, Guangdong, China). Rats were fed under specific conditions, at a humidity of 50–60%, a temperature of 22 ± 24 °C and a 12-h day/night cycle. All rats were permitted with free access to feed and water.

To establish an OA rat model, the rats were subject to anterior cruciate ligament (ACL)/medial collateral ligament (MCL) transection. The rats were fasted for 8 h prior to operation with access to water. Afterwards, the rats were anesthetized via intraperitoneal injection of 3% pentobarbital sodium (0.4 mL/100 g; P3761, Sigma, St. Louis, MO, USA). The double knee joints of the hind limb were incised along the medial edge of the patellar ligament. After the joint capsule was exposed, the ACL and MCL were transected and the medial meniscus was removed. The incision was sutured post-operation, followed by anti-infective and analgesia management. The OA rat models were assessed after 2 weeks. Besides, eight rats were sham-operated as control, whose double knee joints were incised along the medial edge of the patellar ligament, followed by a series of procedures as indicated above, without ACL/MCL transection.

Identification of BM-MSCs

BM-MSCs were isolated and cultured using the whole bone marrow adherence method. Rats were anesthetized via intraperitoneal injection of 3% pentobarbital sodium and then sterilized in 75% ethanol for 5 min. The bilateral femora and tibia were isolated under aseptic conditions and the metaphysis was opened to expose the medullary cavity. Then, rat bone marrow was harvested through washing with low glucose-Dulbecco's modified Eagle's medium (L-DMEM). Next, the bone marrow was centrifuged at 1000 r/min for 5 min with the supernatant discarded. The precipitation was resuspended with L-DMEM containing 10% fetal bovine serum (FBS). The cell suspension was inoculated at a density of 1×10^6 cells/mL and incubated in a 5% CO₂ incubator at 37 °C. Half of the medium

was changed after incubation for 24 h. The cells were then cultured with medium changed every 2 days. Cells were passaged at a confluence level of 80–90%, at a ratio of 1:2. Morphology of BM-MSCs was observed under an inverted microscope.

BM-MSCs at passage 2 were collected and adjusted to a cell concentration of 1×10^6 cells/mL. BM-MSCs at passage 2 were incubated with fluorescein isothiocyanate (FITC)-labeled monoclonal antibodies against CD34, CD45, CD29, or CD90 for 1 h and then detected on a flow cytometer.

Isolation and identification of BM-MSC-derived exosomes

The BM-MSCs at passage 2 were cultured in DMEM medium supplemented with exosome-free FBS for 24 h. The cells were then collected and centrifuged at 300g, 2000g and 10,000g for 5 min, 10 min and 35 min respectively. After that, the supernatant was filtered using a 0.22- μ m filter membrane (Merck Millipore, Tullagreen, Ireland), followed by ultracentrifugation and centrifugation both at 100,000g for 2 h respectively. All ultracentrifugation steps were performed at 4 °C in a Beckman ultracentrifuge (Optima L-90K) with a SW-32Ti rotor and low-speed centrifugation steps were adopted in a Beckman Coulter Centrifuge (Allegra X-15R). Exosomes were finally resuspended at 50–100 μ L phosphate buffer saline and stored at –80 °C for further experiments.

For Western blot analysis, the isolated exosomes (20 mL) were lysed with 300 μ L lysis buffer on ice for 30 min and centrifuged at 10000 r/min and 4 °C for 5 min. The supernatant was collected and the protein concentration was measured using the bicinchoninic acid (BCA) method. A total of 30 μ g total protein was separated by sodium dodecyl sulfate-polyacrylamide gel electrophoresis (SDS-PAGE) and transferred onto the polyvinylidene fluoride (PVDF) membrane. After blocking in 5% skim milk at 37 °C for 2 h, the membrane was incubated with antibodies against CD9, TSG101, calnexin and CD63, which were all diluted at 1:1000 overnight at 4 °C. The next day, the membrane was incubated with horseradish peroxidase (HRP)-labeled immunoglobulin G (IgG) (1:1000) at 37 °C for 2 h. Finally, the membrane was colored by the enhanced chemiluminescence (ECL) method and exposed under dark conditions.

Dual-luciferase reporter assay

The bioinformatics prediction website (<http://mirtarbase.mbc.nctu.edu.tw/php/search.php>) was used to predict the miR-9-5p binding sites in the 3'untranslated region (3'UTR) of SDC1. Primarily, the full length of complementary DNA (cDNA) and 3'UTR fragment of SDC1 were cloned into the pmirGLO vector (E1330, Promega, Madison, WI, USA), namely pSDC1-wild type (Wt). The pSDC1-mutant (Mut) was

constructed, in which the potential binding sites of miR-9-5p on pSDC1-Wt were mutated. The pSDC1-Wt/Mut was separately co-transfected with miR-9-5p mimic or negative control (NC) into 293T cells (CRL-1415, ATCC, Manassas, VA, USA). The renilla luciferase expressing pRL-TK vector (E2241, Promega, Madison, WI, US) served as internal control and luciferase activity was tested using the Glomax20/20 luminometer (Promega, WI, USA).

Animal treatment

The rats with OA-like damage were administrated with MSC-derived exosomes, the exosomes carrying miR-9-5p mimics (exo-miR-9-5p mimic), miR-9-5p inhibitors (exo-miR-9-5p mimic), or their NCs (exo-mimic-NC and exo-inhibitor NC), or miR-9-5p-embedded liposomes (liposomes miR-9-5p) into the joint cavity of the left hind limb ankle joint. To alter the SDC1 expression in rats with OA-like damage, they were injected with SDC1 overexpression-embedded liposomes (SDC1 vector) or its control NC vector. The miR-9-5p inhibitors (anti-miR-9-5p) and miR-9-5p mimics (miR-9-5p) were synthesized by Shanghai GenePharma Co., Ltd. (Shanghai, China). miR-9-5p mimic; 5'-CGAGCTCTGTGTGTGTGTGTGTGTG-3'; miR-9-5p inhibitor; -TTCCGCGGCCGCTATGGCCGACGTCGACGGGAATGGGGAAAGGGAA-3'. The miR-9-5p mimics, inhibitors, or their NCs (100 pmol; Genepharma Co., Ltd., Shanghai, China) were diluted in 250 μ L serum-free medium and then transfected into the BMSCs with addition of 10 μ L Lipofectamine® 2000 (diluted in 250 μ L serum-free medium), followed by incubation for 4 h at 37 °C. This was then further cultured in a complete medium for another 48 h. BMSCs were collected and exosomes were isolated after reverse transcription quantitative polymerase chain reaction (RT-qPCR) determination of transfection efficiency. The exosomes isolated were used in further experiments.

Classification of the severity of OA lesions of cartilage

Seven weeks after modeling, the rats were sacrificed by cervical dislocation after anesthesia. Articular cartilages were collected from sham-operated rats and rats with OA-like damage were then injected with exosomes. After a series of routine fixation, decalcification and embedding, the histopathological changes of tissue sections were observed under an optical microscope after HE staining. Afterwards, the tissue sections were scored based on Mankin scores (Table 1) for classification of the severity of OA lesions. The nitric oxide (NO), superoxide dismutase (SOD), nitric oxide synthase (iNOS) and malonaldehyde (MDA) in synovial fluid were detected using nitrate reductase assay, xanthine oxidase assay and colorimetric thiobarbituric acid (TBA) method respectively.

Table 1 Mankin score for classification of the severity of OA lesions of the articular cartilage. OA, osteoarthritis

Indicators
The cartilage surface is light blue or colorless and translucent
The cartilage surface softens but still smooth
The cartilage is thinner with the emergence of small fiber bundles
The cartilage shows obvious fibrous bundles
The cartilage has abrasive fibrous bundle with subchondral bone exposure and osteosclerosis

Hematoxylin-eosin staining

The articular cartilage tissues were fixed in 4% paraformaldehyde for 24 h, dehydrated with gradient ethanol, paraffin-embedded and sliced into 5- μ m sections. Following dewaxing and hydration, the sections were stained with hematoxylin (Beijing Solarbio Science & Technology Co., Ltd., Beijing, China) for 2 min, washed under running water for 10 s and differentiated by 1% hydrochloric acid alcohol for 10 s. Afterwards, the sections were stained with eosin solution for 1 min. The sections were then dehydrated, cleared and mounted with neutral gum. Morphological changes of articular cartilage tissues were observed under an optical microscope (XP-330, Shanghai Bingyu Optical Instrument Co., Ltd., Shanghai, China). The experiment involved at least 3 wells, each repeated in triplicate.

Immunohistochemistry

The articular cartilage tissues were fixed in 4% paraformaldehyde for 24 h. Then, the tissues were dehydrated with gradient ethanol, paraffin-embedded and sliced into 5- μ m sections. After being dewaxed, the tissue sections were dehydrated by gradient ethanol, immersed in 3% H₂O₂ for 10 min, followed by high-pressure antigen retrieval for 90 s. Afterwards, the sections were blocked with 100 μ L 5% bovine serum albumin (BSA) solution at 37 °C for 30 min. The sections were then incubated with 100 μ L rabbit anti SDC1 (1:500, ab128936, Abcam, Cambridge, MA, USA) overnight at 4 °C. The next day, the sections were incubated with biotin-labeled secondary antibody goat anti-rabbit (HY90046, Shanghai Hengyuan Biotechnology Co., Ltd., Shanghai, China) at 37 °C for 30 min. Then, the sections were incubated with streptavidin-peroxidase (Beijing Zhongshan Biotechnology Co., Ltd., Beijing, China) at 37 °C for 30 min and colored by diaminobenzidine (DAB) (Bioss Biotech, Beijing, China) at room temperature. Finally, the sections were counterstained by hematoxylin for 5 min, differentiated by 1% hydrochloric acid alcohol for 4 s and blued under running water for 20 min. The SDC1 positive cells were analyzed using Image-Pro Plus image

analysis software (Media Cybernetics, Silver Springs, MD, USA). The brownish-yellow colored cells were considered as positive cells (Kelkar et al. 2017). Five high-power fields ($\times 200$) were randomly selected from each section, with 100 cells counted in each field. The percentage of positive cells = the number of positive cells/the number of total cells and the percentage of positive cells > 10% was regarded as positive (+), < 10% as negative (-). The experiment was repeated three times independently.

Enzyme-linked immunosorbent assay

ELISA was carried out strictly in accordance with the instructions of the ELISA kit (eBioscience, San Diego, CA, USA). The levels of inflammatory factors, oxidative stress biomarkers and OA-related factors in joint fluid of rats were determined using the ELISA kit with the following antibodies (Abcam, Cambridge, MA, USA): interleukin-6 (IL-6; 1:1000, ab234570), interleukin-1 β (IL-1 β ; 1:1000, ab100768), tumor necrosis factor- α (TNF- α ; 1:1000, ab6671), C-reactive protein (CRP; 1:20000, ab108827), cyclooxygenase-2 (COX2; 1:20000, ab52237) and alkaline phosphatase (AKP; Tongwei Reagent Co., Ltd., Shanghai, China). The optical density (OD) values of each well were detected using the versatile microplate reader at 450 nm (Synergy 2, Biotek, Winooski, VT, USA).

RNA isolation and quantitation

Total RNA in the articular cartilage tissues was extracted according to the instructions of the Trizol kit (15596-026, Invitrogen, Gaithersburg, MD, USA). Then, the extracted RNA was reversely transcribed into complementary DNA (cDNA) based on the manufacturer's protocols provided by the reverse transcription kit (K1621, Fermentas, Maryland, NY, USA). Quantitative PCR was performed using the fluorescent quantitative real-time PCR kit (Takara, Dalian, China) on a real-time PCR instrument (ABI7500, ABI, Foster City, CA, USA), with β -actin used as the internal reference. The fold changes were calculated by means of relative quantification ($2^{-\Delta\Delta Ct}$ method): $\Delta\Delta Ct = (\text{mean Ct value of the target gene in the experimental group} - \text{mean Ct value of the housekeeping gene in the experimental group}) - (\text{mean Ct value of the target gene in the control group} - \text{mean Ct value of the housekeeping gene in the control group})$. Primer sequences for miR-9-5p, SDC1, matrix metalloproteinase-13 (MMP-13), osteocalcin (OCN), cartilage oligomeric matrix protein (COMP) and β -actin were designed and synthesized by Shanghai Genechem Co., Ltd. (Shanghai, China) (Table 2). The aforementioned method was applicable in an equal fashion to the detection among the cells.

Table 2 Primer sequences for RT-qPCR

Gene	Sequence (5'-3')
miR-9-5p	F: GCGTCTTTGGTTATCTAGCTGTA R: GCGAGCACAGAATTAATACGAC
SDC1	F: GAGAGGAATCCGGCAGTAGA R: GAGCCATCTTGATCTTCAGG
MMP-13	F: CCCTGGAGCCCTGATGTTT R: CTCTGGTGTTTTGGGGTGCT
OCN	F: CATGAGAGCCCTCACA R: AGAGCGACACCCTAGAC
COMP	F: GCAGATGCTTCGGGAAGTCA R: TTGATGCACACGGAGTTGGGG
β -actin	F: GGAGATTACTGCCCTGGCTCCTA R: GACTCATCGTACTCCTGCTTGCTG
U6	F: AATTGGAACGATACAGAGAAGATTAGC R: TATGGAACGCTTACGAATTTG

RT-qPCR, reverse transcription quantitative polymerase chain reaction; *miR-9-5p*, microRNA-9-5p; *F*, forward; *R*, reverse; *SDC1*, syndecan-1; *MMP-13*, matrix metalloproteinases-13; *OCN*, osteocalcin; *COMP*, cartilage oligomeric matrix protein; *U6*, small nuclear RNA

Western blot analysis

Total protein in articular cartilage tissues was extracted, separated by SDS-PAGE and transferred onto a nitrocellulose membrane. Following that, the membrane was blocked in 5% skim milk at room temperature for 1 h. The membrane was then probed with the primary antibodies (Abcam, Cambridge, MA, USA) against SDC1 (1:1000, ab128936), MMP-13 (1:3000, ab39012), OCN (1:10000, ab13420), COMP (1:10000, ab74524) and glyceraldehyde 3-phosphate dehydrogenase (GAPDH; ab8245) at 4 °C overnight. Following that, the membrane was incubated with HRP-labeled goat anti-rabbit IgG (1:1000, Wuhan Boster Biological Technology Co., Ltd., Wuhan, Hubei, China) at 37 °C for 1 h. Subsequently, ECL reaction solution (Pierce, Waltham, MA, USA) was used to develop the membrane at room temperature for 1 min. The relative protein level was presented by the ratio of the gray value of the target band to that of the internal reference band, with GAPDH as an internal reference.

Statistical analysis

Statistical analyses were performed using SPSS 21.0 statistical software (IBM, Armonk, NY, USA). Measurement data were presented as mean \pm standard deviation. Differences in intergroup settings were evaluated by unpaired *t* test. A *p* value < 0.05 indicated statistical significance.

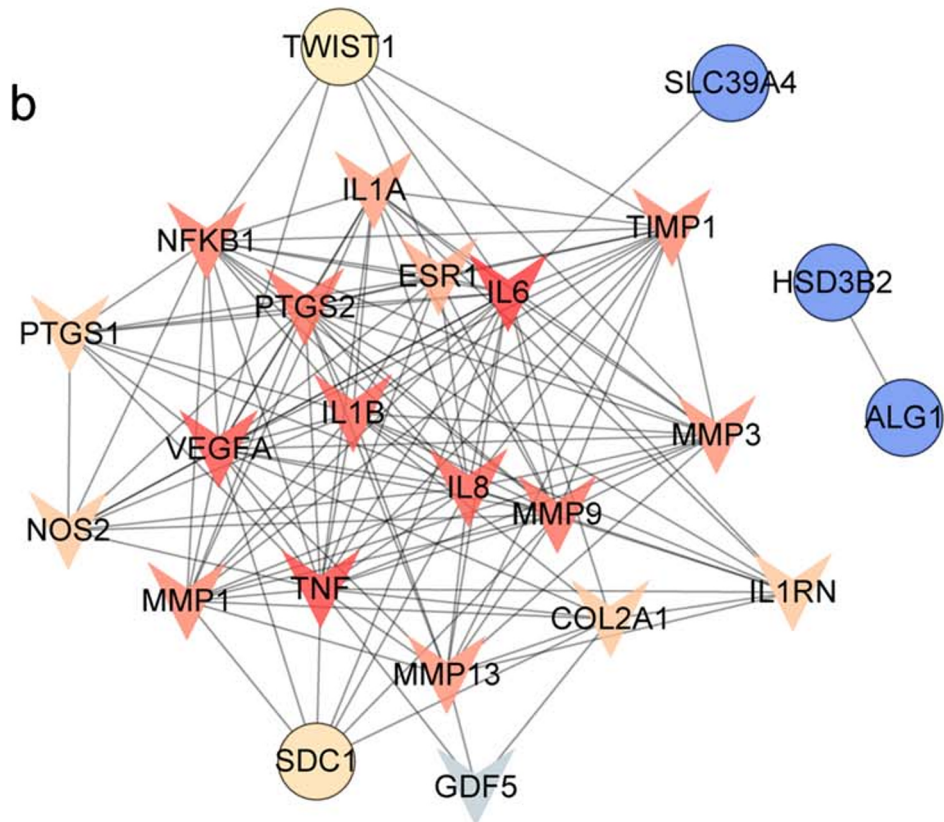
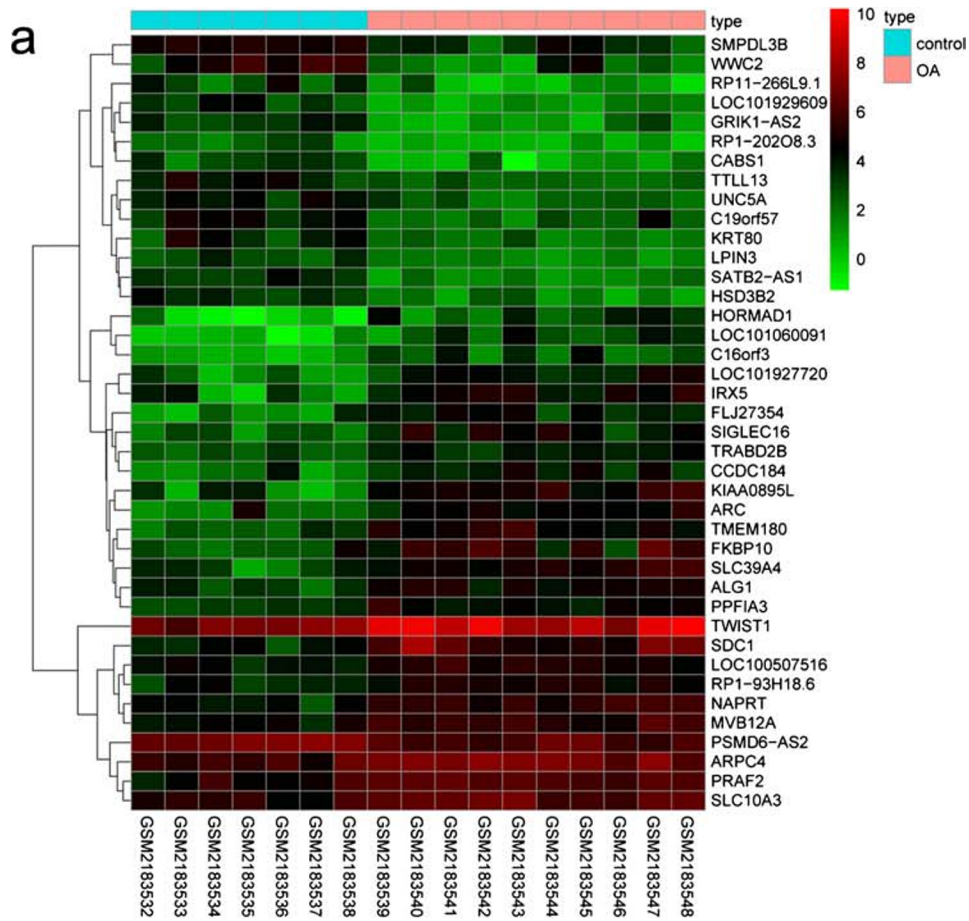
Results

miR-9-5p might be involved in OA via regulation of SDC1

Differential analysis was performed on OA GSE82107 microarray data using the R language in order to screen DEGs and the heat map of expression of the top 40 DEGs with the largest fold change between OA and control was drawn (Fig. 1a). The known OA-related genes were retrieved from the DiGSeE database and the top 20 genes (IL1B, TNF, PTGS2, IL6, MMP-3, MMP-1, OAP, IL8, NFKB1, IL1RN, MMP-13, TIMP1, PTGS1, COL2A1, ESR1, GDF5, NOS2, IL1A, VEGFA, MMP-9) were used as disease genes. Subsequently, the screened 40 DEGs and selected 20 disease genes were then included in the String database to construct a gene-gene interaction network (Fig. 1b), from which SDC1 was suggested to be a DEG that interacted with most of the disease genes. As shown in Fig. 1(a), SDC1 had a higher expression in OA synovial tissues than in the normal synovial tissues. Therefore, SDC1 was selected as a candidate gene for subsequent analyses. Next, the putative miRNAs with the potential to regulate SDC1 were predicted from TargetScan database. Consequently, 8 miRNAs were found to have conserved binding sites (Table 3). Among the 8 miRNAs, miR-9 has been already suggested to exhibit a low expression in OA (Gu et al. 2016; Song et al. 2013). Additionally, miR-9 could also be released from exosomes (Lu et al. 2018). Therefore, we speculate that exosomal miR-9-5p might influence OA progression by regulating SDC1.

Successful establishment of OA rat models

The sham-operated rats and the rats received operation with ACL/MCL transection to induce OA-like damage were allowed to recover for 2 weeks after operation. A full examination has been conducted to assess their health conditions. Examination showed that they were all infection-free and that they were able to move normally. Articular cartilage of those rats were collected and observed under the optical microscope 7 weeks after operation. In the sham-operated rats, some part of cartilage surface lost luster but was still smooth and the cartilage became thicker without presence of marginal osteophyte. In the rats that received operation with ACL/MCL transection, the cartilage surface was reddish, lost luster and was unsmooth, accompanied with emergence of abrasive fascicular fiber degeneration and cartilage defects, as well as formation of marginal osteophytes and infiltration of a large number of inflammatory cells. The cartilage injury was more severe in the rats that received operation with ACL/MCL transection than in the sham-operated rats. As suggested, rats received operation with ACL/MCL transection exhibited OA-like damage.



◀ **Fig. 1** SDC1 was suggested to be a DEG in OA synovial tissues that interacted with most of the disease genes. **a** Heat map of the top 40 DEGs with the largest fold change obtained from the GSE82107 chip. The horizontal coordinate represents the samples and the vertical coordinate represents the genes. The upper-right histogram is the color gradation. Each rectangle corresponds to one gene expression in one sample. **b** Gene-gene interaction network of DEGs and known disease genes. Circle presents DEGs and the arrow represents disease genes. The genes that have no interaction with other genes are not shown in panel **b**

Observation score and Mankin score were applied to assess the severity of OA lesion 7 weeks after operation, which suggested that both observation score and Mankin score of cartilage were notably increased in the rats with OA-like damage compared with the sham-operated rats ($p < 0.05$) (Fig. 2a). Furthermore, HE staining was performed for histological observation of cartilage tissues. As shown in Fig. 2(b), in the sham-operated rats, smooth cartilage surface and normal cartilage structure without defects were observed. The articular chondrocytes were arranged in a neat order with mild hyperplasia or decreases and the tidal line was complete. In the rats with OA-like damage, the cartilage presented with an abrasive and defective surface, which was covered by fibrous necrotic tissues and the normal cartilage structure disappeared. Moreover, the number of articular chondrocytes was significantly reduced; which were swollen, necrotic and disintegrated and the tidal line vanished. Based on the results mentioned above the OA model was successfully established in the rats.

Successful isolation of BM-MSC-derived exosomes

BM-MSCs were isolated and suspended. After 24 h, some adherent cells could be observed under the inverted microscope. These cells were observed to be round-shaped with different sizes. Then, the number of adherent cells gradually increased from 4 to 5 days of culture and cellular colonies were formed, which were either in polygonal or fusiform shapes. On the 10th day, cells reached 90% confluence and were passaged. After

passage 2, the cells were mainly spindle-shaped, distributed in an eddy-like structure and radial in form, which was the typical morphology of BM-MSCs (Fig. 3a, a'). The BM-MSCs at passage 3 were subjected to flow cytometry for detection of BM-MSC surface markers (CD29, CD90, CD34 and CD45). As shown in Fig. 3(b, b', b''), a high expression of CD29 (98.23%) and CD90 (75.84%) and a low expression of CD34 (0.081%) and CD45 (0.82%) were observed, suggesting the successful isolation of BM-MSCs.

Furthermore, exosomes were derived from BM-MSCs and were observed under TEM. Exosomes exhibited a uniform size with 40–100 nm in diameter. Moreover, they showed either a round or tea-shaped morphology and the outer membrane was complete with low electron density (Fig. 3c). Western blot analysis was employed to confirm the expression of the exosome surface marker, which showed that CD9, TSG101 and CD63 were positively expressed in exosomes isolated from BM-MSCs and the integral endoplasmic reticulum protein, calnexin, was not expressed (Fig. 3d). As a result, BM-MSC-derived exosomes were successfully isolated.

BM-MSC-derived exosomes alleviate OA in rats

To investigate whether BM-MSC-derived exosomes would alleviate OA in rats, one side of the knee joint of rats with OA-like damage was injected with BM-MSC-derived exosomes, with normal saline into the other side as a control. The OA lesions were assessed according to observation score and Mankin score of cartilage at the 7th week after injection. Next, HE staining was applied to observe the histological morphology of cartilage. ELISA was employed to determine the levels of inflammatory factors (IL-1, IL-6, TNF- α , and CRP) and AKP content as well as oxidative stress injury indicators (NO, MDA, iNOS, COX2 and SOD) in the synovial fluid. RT-qPCR and western blot analysis were further conducted to determine the mRNA and protein expression of OA-related factors (MMP-13, COMP and OCN) in articular cartilage tissues.

Table 3 Prediction of candidate miRNAs to regulate SDC1 through TargetScan

miRNA	Position in the UTR	Seed match	Context ++ score	Context ++ score percentile	Weighted context ++ score	Conserved branch length	Pct
mo-miR-19b-3p	488–495	8mer	–0.38	96	–0.38	5.2	0.85
mo-miR-19a-3p	488–495	8mer	–0.38	96	–0.38	5.2	0.85
mo-miR-9a-5p	1115–1121	7mer-1A	–0.16	86	–0.16	4.815	0.76
mo-miR-105	376–383	8mer	–0.42	99	–0.42	4.966	0.75
mo-miR-291a-3p	376–383	8mer	–0.36	98	–0.36	4.966	0.75
mo-miR-10a-5p	724–731	8mer	–0.37	98	–0.37	4.368	0.67
mo-miR-212-5p	1432–1438	7mer-m8	–0.19	86	–0.11	3.872	0.14
mo-miR-665	998–1005	8mer	–0.34	97	–0.34	2.618	N/A

miR, microRNA; UTR, untranslated region; SDC1, syndecan-1

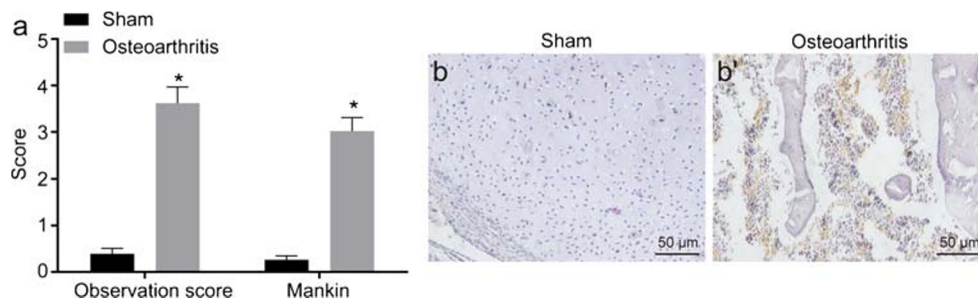


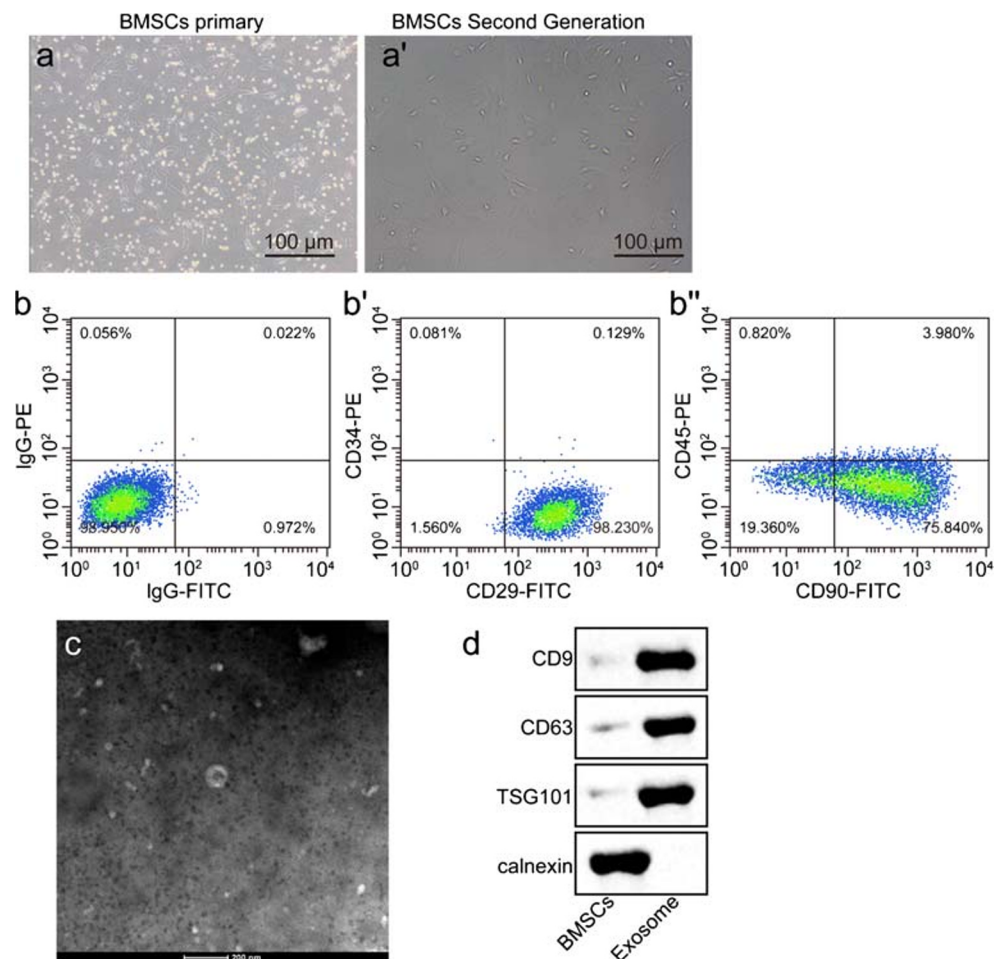
Fig. 2 Successful establishment of OA rat models. **a** The observation score and Mankin score of cartilage in sham-operated rats and rats that received operation with ACL/MCL transection to induce OA. **b** HE staining of cartilage from sham-operated rats. **b'** HE staining of cartilage from the rats that received operation with ACL/MCL transection ($\times 200$).

* $p < 0.05$ vs. the sham-operated rats. The data were measurement data and expressed by mean \pm standard deviation. If departure from normality and homogeneity of variance was not observed, a data comparison between the two groups was performed using unpaired t test. $N = 8$

As shown in the results of HE staining in Fig. 4(a,a') the injured area of knee joint injected with normal saline in the rats with OA-like damage with disordered structure showed infiltration of a large number of inflammatory cells, while the knee joint injected with exosome continuously in a clear structure showed infiltration of few inflammatory cells. The observation score as well as Mankin score was significantly lower in the cartilage of rats injected with exosome than that in the cartilage of rats injected with normal saline (Fig. 4b)

($p < 0.05$), suggesting the alleviation of cartilage injury. The results of ELISA showed relative lower levels of IL-1, IL-6, TNF- α and CRP and AKP content (Fig. 4c, d) in the synovial fluid of knee joint injected with exosome compared with those in the synovial fluid of the knee joint injected with normal saline ($p < 0.05$), demonstrating protection of exosome against cartilage inflammation. The levels of NO, MDA, iNOS and COX2 were markedly decreased in the synovial fluid of the knee joint injected with

Fig. 3 Successful isolation of BM-MSCs-derived exosomes. **a** Morphology of BM-MSCs at passage 0 observed under an inverted microscope ($\times 100$). **a'** Morphology of BM-MSCs at passage 2 observed under an inverted microscope ($\times 100$). **b** Expression of IgG detected by flow cytometer. **b'** Expression of BM-MSCs surface marker (CD29) detected by flow cytometer. **b''** Expression of BM-MSCs surface marker (CD90) detected by flow cytometer. **c** BM-MSCs-derived exosomes observed under TEM. **d** Expression of exosome surface markers measured by Western blot analysis



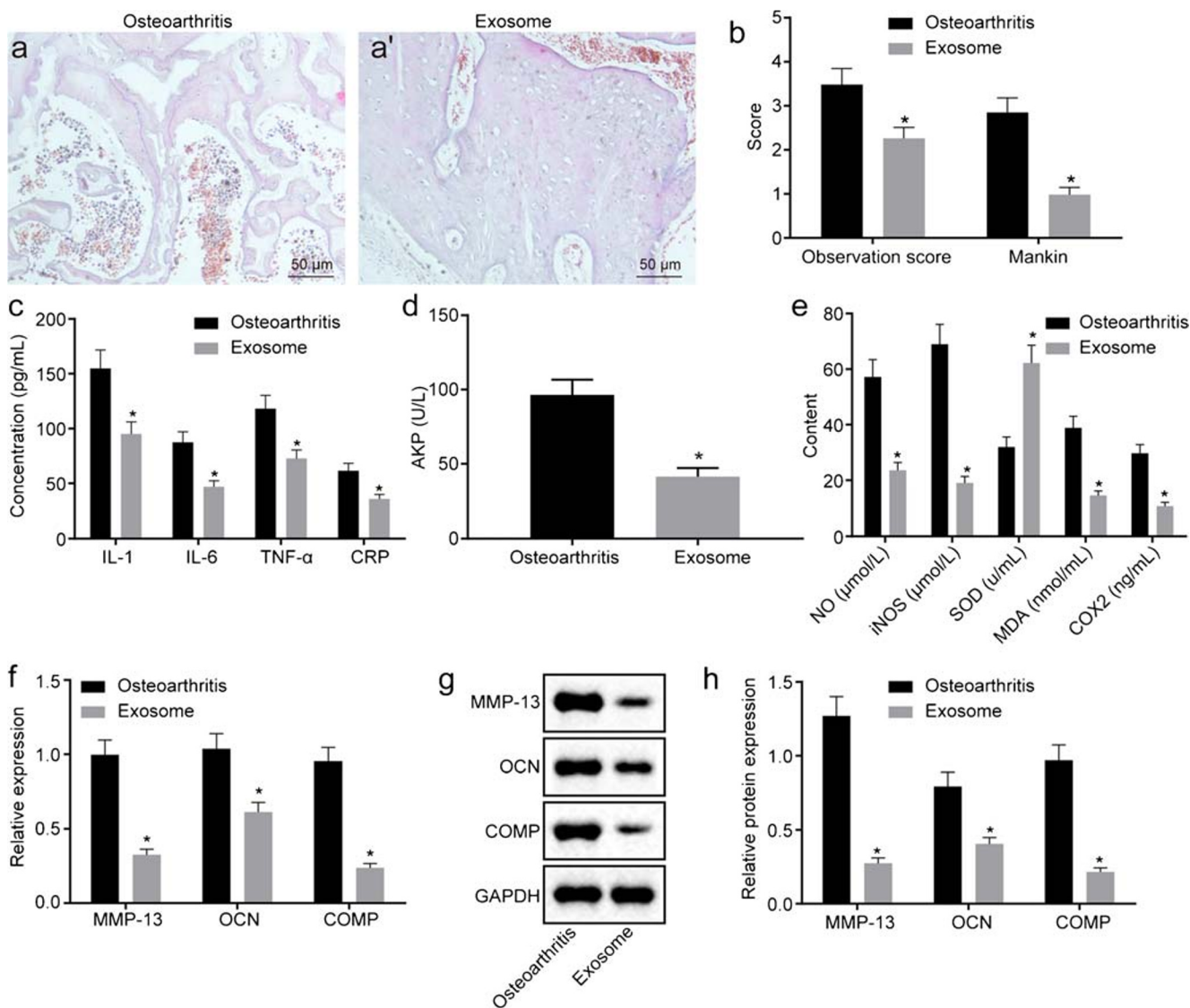


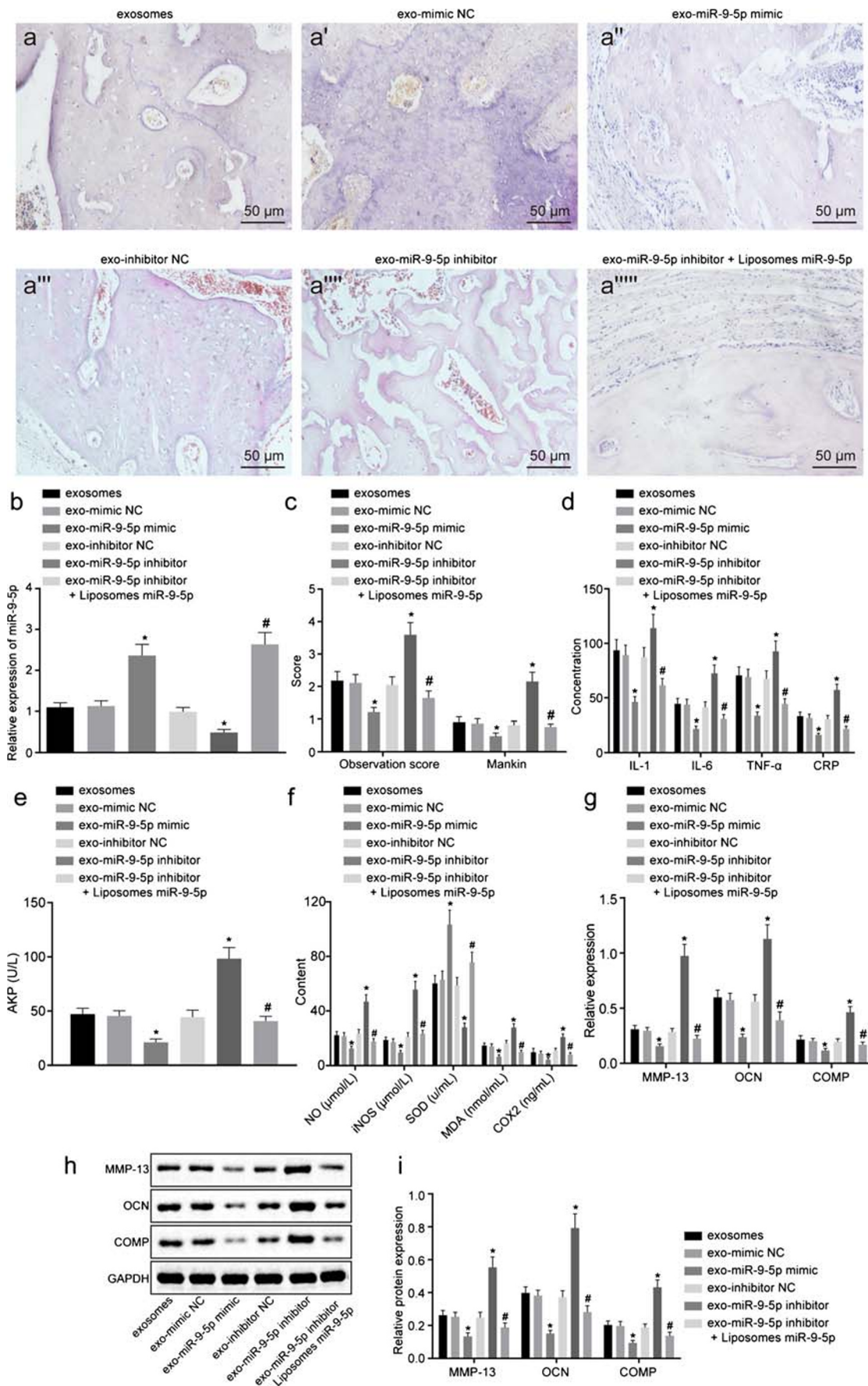
Fig. 4 Cartilage injury and inflammation were rescued in rats with OA-like damage by injection with BM-MSC-derived exosomes. **a** HE staining of cartilage from rats with OA-like damage ($\times 200$). **a'** HE staining of cartilage from OA rats injected with BM-MSC-derived exosomes ($\times 200$). **b** Observation score and Mankin score of cartilage. **c** Levels of inflammatory factors (IL-1, IL-6, TNF- α and CRP) in joint fluid evaluated by ELISA. **d** Content of AKP in synovial fluid determined by ELISA. **e** Contents of oxidative stress injury indicators (NO, MDA, iNOS, COX2 and SOD) in synovial fluid measured by ELISA. **f** mRNA expression of OA-related factors (MMP-13, COMP and OCN) determined by RT-qPCR. **g, h** Protein levels of MMP-13, COMP and OCN assessed by Western blot analysis. * $p < 0.05$ vs. rats with OA-like damage. The data were measurement data and expressed by mean \pm standard deviation. If departure from normality and homogeneity of variance was not observed, a data comparison between the two groups was performed using unpaired t test. $N = 8$

iNOS, COX2 and SOD) in synovial fluid measured by ELISA. **f** mRNA expression of OA-related factors (MMP-13, COMP and OCN) determined by RT-qPCR. **g, h** Protein levels of MMP-13, COMP and OCN assessed by Western blot analysis. * $p < 0.05$ vs. rats with OA-like damage. The data were measurement data and expressed by mean \pm standard deviation. If departure from normality and homogeneity of variance was not observed, a data comparison between the two groups was performed using unpaired t test. $N = 8$

exosome versus the synovial fluid of the the knee joint injected with normal saline ($p < 0.05$) (Fig. 4e, f). Furthermore, a decline in the expression of MMP-13, OCN and COMP mRNA and protein while an elevation of SOD mRNA and protein was observed in the articular cartilage tissues removed from rats injected with exosome in comparison with those removed from rats injected with normal saline ($p < 0.05$) (Fig. 4g, h). All the results above led to a conclusion that BM-MSC-derived exosomes were capable of inhibiting OA progression, as evidenced by alleviated cartilage injury and inflammation.

BM-MSC-derived exosomal miR-9-5p ameliorates OA in rats

The results mentioned above demonstrated that the cartilage injury and inflammation in keen joints of OA rats were improved after injection of BM-MSC-derived exosomes. It has been reported that miR-9-5p could protect against rheumatoid arthritis (Li et al. 2019). To better elucidate its mechanism, we overexpressed or inhibited the miR-9-5p in exosomes and delivered them into the joint cavity of the left hind limb ankle joint of OA rats.



◀ **Fig. 5** Cartilage injury and inflammation of OA were attenuated by exosomal miR-9-5p. **a** HE staining of cartilage from OA rats injected with exosomes ($\times 200$). **a'** HE staining of cartilage from OA rats injected with exo-mimic NC ($\times 200$). **a''** HE staining of cartilage from OA rats injected with exo-miR-9-5p mimic ($\times 200$). **a'''** HE staining of cartilage from OA rats injected with exo-inhibitor NC ($\times 200$). **a''''** HE staining of cartilage from OA rats injected with exo-miR-9-5p inhibitor ($\times 200$). **a'''''** HE staining of cartilage from OA rats injected with exo-miR-9-5p inhibitor + liposomes miR-9-5p ($\times 200$). **b** miR-9-5p expression in cartilage tissues determined by RT-qPCR. **c** Observation score and Mankin score of cartilage. **d** Levels of inflammatory factors (IL-1, IL-6, TNF- α and CRP) in joint fluid evaluated by ELISA. **e** Content of AKP in synovial fluid determined by ELISA. **f** Contents of oxidative stress injury indicators (NO, MDA, iNOS, COX2 and SOD) in the synovial fluid measured by ELISA. **g** mRNA expression of OA-related factors (MMP-13, COMP and OCN) in articular cartilage tissues determined by RT-qPCR. **h, i** Protein levels of MMP-13, COMP and OCN assessed by Western blot analysis. * $p < 0.05$ vs. rats with OA-like damage injected with exosomes; # $p < 0.05$ vs. rats with OA-like damage injected with exo-miR-9-5p inhibitor. The data were measurement data and expressed by mean \pm standard deviation. If departure from normality and homogeneity of variance was not observed a data comparison between the two groups was performed using unpaired t test. $N = 8$

Following injection, cartilage was removed from rats and subjected to HE staining for pathological observation. As depicted in Fig. 5(a–a'''''), less OA infiltration with relatively more consecutive tissues and a clearer structure were observed in the rats injected with MSC-derived exosomes, exo-mimic NC and exo-inhibitor NC. It was also observed that the cartilage injury was improved in response to exo-miR-9-5p mimic and exacerbated in response to exo-miR-9-5p inhibitor, when compared with exo-mimic NC. The miR-9-5p expression in cartilage tissues of rats following the delivery of exosomes was determined by RT-qPCR (Fig. 5b). An increase in miR-9-5p expression was found in the rats injected with exo-miR-9-5p mimic. Moreover, miR-9-5p was decreased in the rats with exo-miR-9-5p inhibitor injection, which was then upregulated by liposomes miR-9-5p injection.

With the aim to analyze the role of miR-9-5p involved in the inflammation and oxidative stress in OA, the severity of OA lesion was assessed by observation score and Mankin score of cartilage and the levels of inflammatory factors (IL-1, IL-6, TNF- α and CRP), AKP content and oxidative stress injury indicators (NO, MDA, iNOS, COX2 and SOD) in the synovial fluid, together with the mRNA and protein expression of OA-related factors (MMP-13, COMP and OCN) in articular cartilage tissues were measured by means of ELISA, RT-qPCR and Western blot analysis respectively (Fig. 5c–i). No significant disparity was seen in rats injected with MSC-derived exosomes, exo-mimic NC and exo-inhibitor NC. Compared with exosome injection, exo-miR-9-5p mimic injection resulted in reduced severe OA lesion and Mankin score of cartilage (Fig. 5c, $p < 0.05$). The same trend was observed in the levels of IL-1, IL-6, TNF- α and CRP, NO, MDA, iNOS and COX2, MMP-13, OCN, COMP

and AKP after exo-miR-9-5p mimic injection (Fig. 5d–i, $p < 0.05$). Besides, increased expression of SOD was observed in response to exo-miR-9-5p mimic, which decreased in response to exo-miR-9-5p inhibitor ($p < 0.05$). Liposomes miR-9-5p could reverse the severity of OA promoted by exo-miR-9-5p inhibitor, thereby promoting the recovery of cartilage injury. Therefore, we could surmise that BM-MSC-derived exosomal miR-9-5p was capable of alleviating OA.

SDC1 is negatively regulated by miR-9-5p

The online prediction website miRTarBase (<http://mirtarbase.mbc.nctu.edu.tw/php/search.php>) was used to predict the potential relationship between SDC1 and miR-9-5p, which was further confirmed by dual luciferase reporter assay. A putative miR-9-5p binding site was found in the SDC1 3'UTR (Fig. 6a). The luciferase activity of the SDC1-Wt was reduced when co-transfected with miR-9-5p mimic while that of SDC1-Mut did not change much (Fig. 6b), suggesting that miR-9-5p could specifically bind to and downregulate SDC1.

Immunohistochemical staining was performed to ascertain whether exosomal miR-9-5p could regulate SDC1 (Fig. 6c–e). SDC1 exhibited a markedly higher positive expression in OA rats in comparison to the sham-operated rats. After exosome injection, the positive expression of SDC1 was decreased in the OA rats. When compared with the corresponding NC injection, SDC1 positive expression reduced in response to exo-miR-9-5p mimic injection and increased in response to exo-miR-9-5p inhibitor injection. The increase of SDC1 positive expression induced by exo-miR-9-5p inhibitor was reduced by liposomes miR-9-5p.

SDC1 overexpression deteriorates OA in rats

As aforementioned, SDC1 was found to be negatively regulated by miR-9-5p. Subsequently, SDC1-vector was introduced into the rats with OA-like damage to overexpress SDC1, to further explore the regulatory mechanism of miR-9-5p-mediated SDC1 on OA. As with the pathological changes in rat articular cartilage tissues observed from HE staining in the rats with OA-like damage treated with NC vector, there was few infiltrated inflammatory cells in the injured area of cartilage tissues and the structure of cartilage tissues was clear and continuous. However, in the rats with OA-like damage treated with SDC1-vector, the cartilage tissues had a disordered structure, with a large number of infiltrated inflammatory cells and a serious arthritis phenotype (Fig. 7a).

The severity of OA lesion was assessed by observation score and Mankin score of cartilage. Compared with OA rats injected with NC plasmid, the cartilage of OA rats

Fig. 6 Exosomal miR-9-5p might reduce the expression of SDC1. **a** Binding sites between miR-9-5p and SDC1 predicted by miRTarBase. **b** Relationship between miR-9-5p and SDC1 verified by luciferase reporter assay. * $p < 0.05$ vs. the cells transfected with NC. **c** Immunohistochemical staining of SDC1 expression in the cartilage tissues of sham-operated rats ($\times 200$, scale bar = 50 μm). **c'** Immunohistochemical staining of SDC1 expression in the cartilage tissues of OA rats ($\times 200$, scale bar = 50 μm). **c''** Immunohistochemical staining of SDC1 expression in the cartilage tissues of OA rats injected with exosomes ($\times 200$, scale bar = 50 μm). **c'''** Immunohistochemical staining of SDC1 expression in the cartilage tissues of OA rats injected with exo-mimic NC ($\times 200$, scale bar = 50 μm). **d** Immunohistochemical staining of SDC1 expression in the cartilage tissues of OA rats injected with exo-miR-9-5p mimic ($\times 200$, scale bar = 50 μm). **d'** Immunohistochemical staining of SDC1 expression in the cartilage tissues of OA rats injected with exo-inhibitor NC ($\times 200$, scale bar = 50 μm). **d''** Immunohistochemical staining of SDC1 expression in the cartilage tissues of OA rats injected with exo-miR-9-5p inhibitor ($\times 200$, scale bar = 50 μm). **d'''** Immunohistochemical staining of SDC1 expression in the cartilage tissues of OA rats injected with exo-miR-9-5p inhibitor + liposomes miR-9-5p ($\times 200$, scale bar = 50 μm). **e** Quantification of SDC1 expression in cartilage tissue; * $p < 0.05$ vs. sham-operated rats; # $p < 0.05$ vs. rats with OA-like damage; & $p < 0.05$ vs. rats with OA-like damage injected with exosomes; % $p < 0.05$ vs. rats with OA-like damage injected with exo-miR-9-5p inhibitor. The data were measurement data and expressed by mean \pm standard deviation. If departure from normality and homogeneity of variance was not observed a data comparison between the two groups was performed using unpaired t test. $N = 8$

plasmid, accompanied by a markedly decreased SOD level and significantly increased levels of NO, MDA, iNOS, COX2, MMP-13, COMP and AKP content (all $p < 0.05$) (Fig. 7c–f). RT-qPCR and Western blot analysis were conducted to measure the mRNA and protein expression of OA-related factors (MMP-13, COMP and OCN) in articular cartilage tissue. The delivery of SDC1 vector was observed to induce a dramatical decrease in MMP-13 and COMP mRNA and protein expression in rats with OA-like damage (Fig. 7g–i) (all $p < 0.05$). These results provided evidence that OA was exacerbated by SDC1 overexpression.

Discussion

The progression of OA shares a close association with progressive destruction of articular cartilage, remodeling of subchondral bone and inflammation of the synovial membrane; however, little is known about the etiology and pathogenesis of OA (Kapoor et al. 2011). Exosomes are important regulators of the intercellular communication and act as potential vehicles for drug and therapeutic genes (Zhang et al. 2017). The present study demonstrated that injection of BM-MSC-derived exosomes into rats with OA-like damage alleviated cartilage injury and inflammation. Consistently, BM-MSC-derived exosomes have been shown to play a positive

role in protecting chondrocytes from apoptosis, preventing macrophages from activation in vitro, as well as inhibiting OA progression in vivo (Cosenza et al. 2017). Our study further showed that exosomal miR-9-5p derived from BM-MSCs alleviated cartilage injury and inhibited inflammation by downregulating SDC1, which in turn contributes to decelerated progression of OA.

Initially, we found that the articular cartilage tissues collected from OA rats who had received an intra-articular injection of exosomal miR-9-5p exhibited a continuous and clear structure, with infiltration of few inflammatory cells, suggesting OA was alleviated. Importantly, miR-9 released from exosomes could suppress angiogenesis in nasopharyngeal carcinoma, suggesting a potential therapeutic role of exosomal miR-9 for the disease (Lu et al. 2018). In a bone matrix gelatin rat model, miR-9 was previously suggested to be a regulator in the process of endochondral ossification (Min et al. 2015). As a matter of fact, the protective role of miR-9-5p has been demonstrated in rheumatoid arthritis induced peripheral neuropathy (Li et al. 2019). A reduction in miR-9 expression has also been reported to give rise to an increased level of its target protogenin; as a result, proliferation and survival of chondroblasts and articular chondrocytes were impeded in OA (Song et al. 2013).

Additionally, decreased levels of IL-1, IL-6, TNF- α and CRP were observed in the synovial fluid of OA rats injected with exosomal miR-9-5p, coupled with elevated SOD as well as decreased levels of NO, MDA, iNOS and COX2. As a consequence, exosomal miR-9-5p contributed to inhibited inflammation and oxidative stress injury. Secreted pro-inflammatory cytokines are important mediators of disturbing OA pathophysiological processes, particularly, IL-1 β and TNF, which were capable of controlling the articular cartilage matrix (Kapoor et al. 2011). The levels of iNOS and COX2 could be induced by IL-1 β , while the reduction of which could effectively suppress inflammatory reaction in OA chondrocytes (Ma et al. 2016). Moreover, miR-9 has been demonstrated to act as an important mediator of oxidative stress in chondrocytes related to OA (D'Adamo et al. 2017). CRP is another critical biomarker for articular cartilage injury or inflammation; its elevation was closely related with the presence of chronic synovial inflammation in patients with idiopathic OA (Gungen et al. 2012).

Apart from that, the expression of MMP-13, OCN, AKP and COMP was downregulated in articular cartilage tissues of OA rat that received an injection of miR-9-5p-contained exosomes. MMP-13 is known as the core factor in the process of OA occurrence and development. According to an aforementioned study, functional experiments have suggested miR-9 as a regulator of the expression of MMP-13 and the content of TNF- α in OA (Min et al. 2015). A decreased expression of miR-9 could drive an enhanced MMP-13 expression in OA cartilage tissues. Lately, MMP-13 expression has been shown

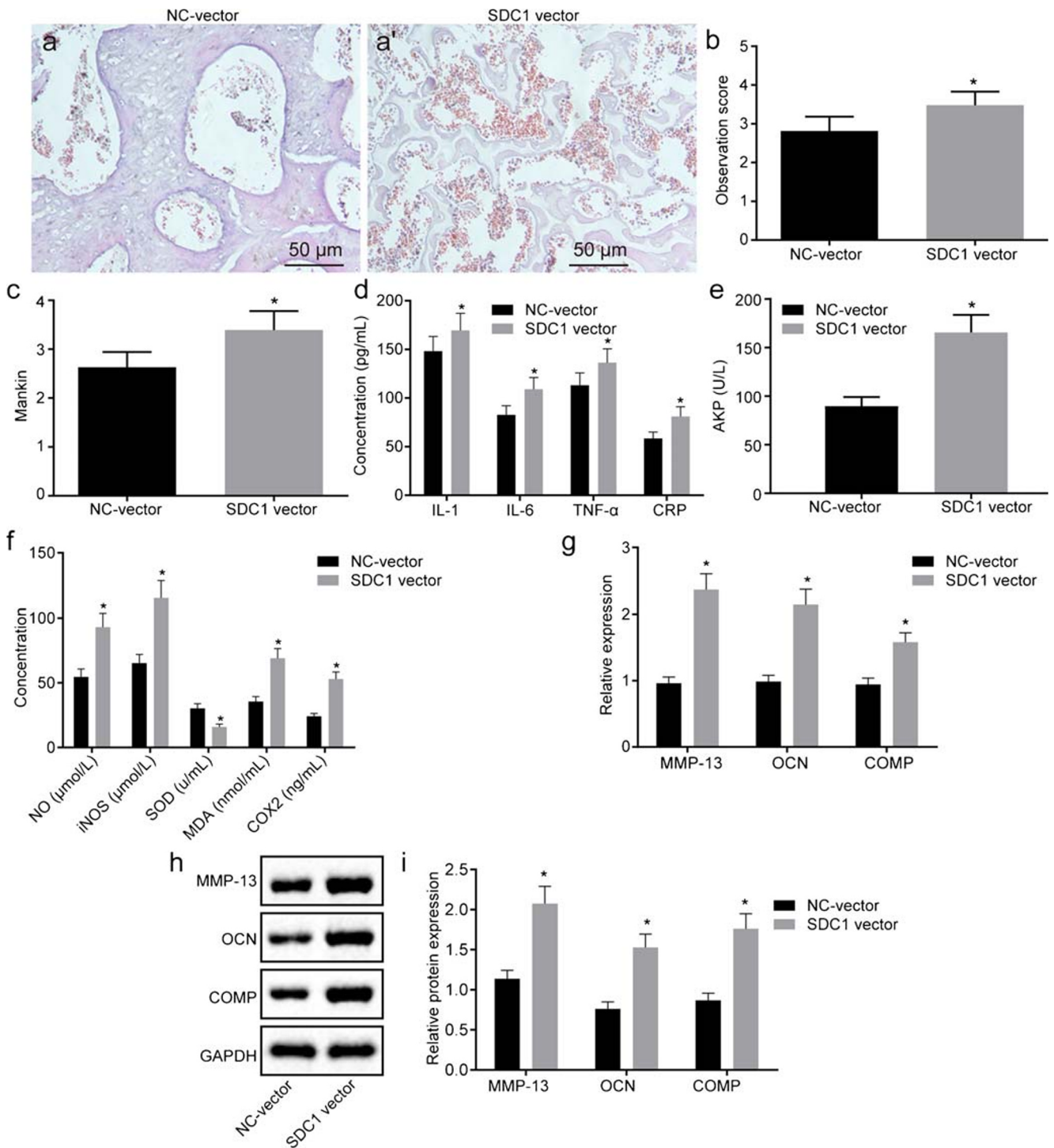
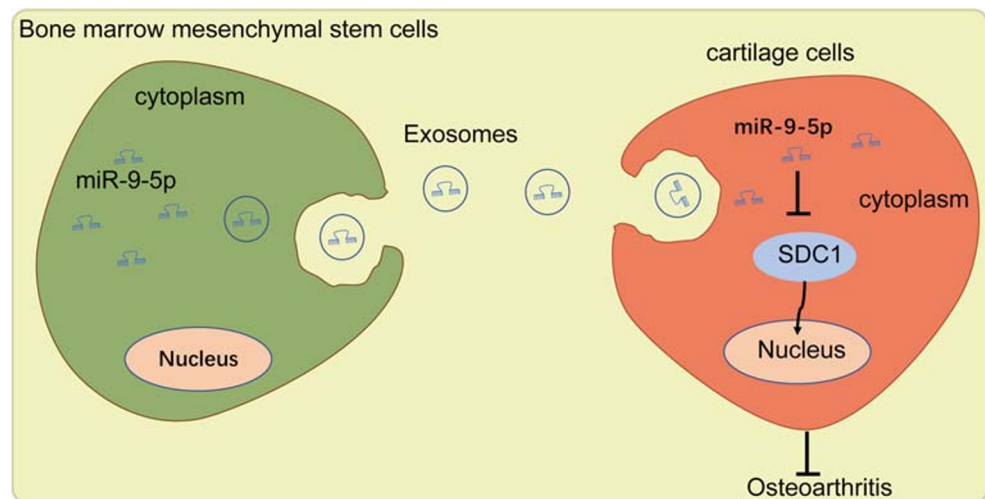


Fig. 7 OA was aggravated by overexpression of SDC1. **a** HE staining of cartilage from OA rats introduced with NC vector ($\times 200$). **a'** HE staining of cartilage from OA rats introduced with SDC1 vector ($\times 200$). **b** Observation score of panels **a** and **a'**. **c** Mankin score of cartilage. **d** Levels of inflammatory factors (IL-1, IL-6, TNF- α and CRP) in synovial fluid evaluated by ELISA. **e** Content of AKP determined by ELISA. **f** Contents of oxidative stress injury indicators (NO, MDA, iNOS, COX2 and SOD) in synovial fluid measured by ELISA. **g**

mRNA expression of OA-related factors (MMP-13, COMP and OCN) determined by RT-qPCR. **h**, **i** Protein levels of MMP-13, COMP and OCN assessed by Western blot analysis. * $p < 0.05$ vs. rats with OA-like damage injected with NC vector. The data were measurement data and expressed by mean \pm standard deviation. If departure from normality and homogeneity of variance was not observed a data comparison between the two groups was performed using unpaired t test. $N = 8$

Fig. 8 The mechanism of BM-MSC-derived exosomal miR-9-5p involved in OA. When miR-9-5p was delivered into chondrocyte from BM-MSC-derived exosomes, miR-9-5p hinders OA progression via downregulation of SDC1



to be depressed by miR-9 overexpression in OA cartilage tissues of rats that had received an injection of miR-9 agomir (Zhang et al. 2018), which is consistent with our results. Serum COMP could be used as an effective biomarker reflecting the progression of OA (Hao et al. 2019). AKP has been found to be significantly amplified in OA bone tissues (Mansell et al. 1997). An osteogenic differentiation assay suggested induction of AKP activity but blunted in vitro matrix mineralization irrespective of the presence of bone sclerosis (Bianco et al. 2018). Also, bone-specific AKP activity is a pathological hallmark predicting the presence of OA (Yamaguchi et al. 2014).

SDC1 was found to be a direct target gene of miR-9-5p and hence was negatively regulated by it. Importantly, cartilage injury and inflammation were induced by SDC1 overexpression in rats with OA-like damage. SDC1 expression was up-regulated in degenerating articular cartilage of OA during the early stage of degeneration (Salminen-Mankonen et al. 2005). Another family member SDC4 was also revealed to serve as a promising target and its suppression may be of a great potential to prevent osteoarthritic cartilage injury in OA (Echtermeyer et al. 2009). Previously, synthetic cannabinoid WIN-55,212-2 mesylate has been illustrated to prevent cartilage breakdown in OA via decreasing the stability of SDC1 (Kong et al. 2016). Therefore, SDC1 is suggested to be involved in OA progression.

Conclusions

All in all, the key findings of the study demonstrate that BM-MSC-derived exosomal miR-9-5p alleviates OA via targeting SDC1 in an OA rat model (Fig. 8). The present findings uncover a role of exosomal miR-9-5p in cartilage injury and inflammation as well as the underlying mechanism, providing a better understanding of the strategy of miRNA delivery in

the treatment of OA. Further studies are required to further illustrate the downstream signaling pathways associated with SDC1 involved in OA.

Acknowledgments We would like to give our sincere appreciation to the reviewers for their helpful comments on this article.

Compliance with ethical standards

Conflict of interest The authors declare that they have no conflicts of interest.

Ethical approval The animal experiments in our study were conducted strictly in accordance with the guidelines of National Institutes of Health (NIH) for animal care and use, with an approval from the Animal Ethics Committee of First Hospital of China Medical University.

References

- Bianco D, Todorov A, Cengic T, Pagenstert G, Scharen S, Netzer C, Hugle T, Geurts J (2018) Alterations of Subchondral bone progenitor cells in human knee and hip osteoarthritis lead to a bone sclerosis phenotype. *Int J Mol Sci* 19:E475
- Chen D, Shen J, Zhao W, Wang T, Han L, Hamilton JL, Im HJ (2017) Osteoarthritis: toward a comprehensive understanding of pathological mechanism. *Bone Res* 5:16044
- Cosenza S, Ruiz M, Toupet K, Jorgensen C, Noel D (2017) Mesenchymal stem cells derived exosomes and microparticles protect cartilage and bone from degradation in osteoarthritis. *Sci Rep* 7:16214
- D'Adamo S, Cetrullo S, Guidotti S, Borzi RM, Flamigni F (2017) Hydroxytyrosol modulates the levels of microRNA-9 and its target sirtuin-1 thereby counteracting oxidative stress-induced chondrocyte death. *Osteoarthr Cartil* 25:600–610
- Echtermeyer F, Bertrand J, Dreier R, Meinecke I, Neugebauer K, Fuerst M, Lee YJ, Song YW, Herzog C, Theilmeier G, Pap T (2009) Syndecan-4 regulates ADAMTS-5 activation and cartilage breakdown in osteoarthritis. *Nat Med* 15:1072–1076
- EL Andaloussi S, Mager I, Breakefield XO, Wood MJ (2013) Extracellular vesicles: biology and emerging therapeutic opportunities. *Nat Rev Drug Discov* 12:347–357

- Gautier L, Cope L, Bolstad BM, Irizarry RA (2004) affy-analysis of Affymetrix GeneChip data at the probe level. *Bioinformatics* 20:307–315
- Gelber AC (2014) In the clinic. Osteoarthritis. *Ann Intern Med* 161:ITC1–IT16
- Glyn-Jones S, Palmer AJ, Agricola R, Price AJ, Vincent TL, Weinans H, Carr AJ (2015) Osteoarthritis. *Lancet* 386:376–387
- Gu R, Liu N, Luo S, Huang W, Zha Z, Yang J (2016) MicroRNA-9 regulates the development of knee osteoarthritis through the NF-kappaB1 pathway in chondrocytes. *Medicine (Baltimore)* 95:e4315
- Gungen G, Ardic F, Findikoglu G, Rota S (2012) The effect of mud pack therapy on serum YKL-40 and hsCRP levels in patients with knee osteoarthritis. *Rheumatol Int* 32:1235–1244
- Hao HQ, Zhang JF, He QQ, Wang Z (2019) Cartilage oligomeric matrix protein, C-terminal cross-linking telopeptide of type II collagen, and matrix metalloproteinase-3 as biomarkers for knee and hip osteoarthritis (OA) diagnosis: a systematic review and meta-analysis. *Osteoarthr Cartil* 27:726–736
- Jo CH, Lee YG, Shin WH, Kim H, Chai JW, Jeong EC, Kim JE, Shim H, Shin JS, Shin IS, Ra JC, Oh S, Yoon KS (2014) Intra-articular injection of mesenchymal stem cells for the treatment of osteoarthritis of the knee: a proof-of-concept clinical trial. *Stem Cells* 32:1254–1266
- Jones IA, Togashi R, Wilson ML, Heckmann N, Vangsnes CT Jr (2019) Intra-articular treatment options for knee osteoarthritis. *Nat Rev Rheumatol* 15:77–90
- Kapoor M, Martel-Pelletier J, Lajeunesse D, Pelletier JP, Fahmi H (2011) Role of proinflammatory cytokines in the pathophysiology of osteoarthritis. *Nat Rev Rheumatol* 7:33–42
- Kelkar MG, Thakur B, Derle A, Chatterjee S, Ray P, De A (2017) Tumor suppressor protein p53 exerts negative transcriptional regulation on human sodium iodide symporter gene expression in breast cancer. *Breast Cancer Res Treat* 164:603–615
- Kong Y, Wang W, Zhang C, Wu Y, Liu Y, Zhou X (2016) Cannabinoid WIN55,2122 mesylate inhibits ADAMTS4 activity in human osteoarthritic articular chondrocytes by inhibiting expression of syndecan1. *Mol Med Rep* 13:4569–4576
- Li Z, Li Y, Li Q, Zhang Z, Jiang L, Li X (2019) Role of miR-9-5p in preventing peripheral neuropathy in patients with rheumatoid arthritis by targeting REST/miR-132 pathway. *In Vitro Cell Dev Biol Anim* 55:52–61
- Lu J, Liu QH, Wang F, Tan JJ, Deng YQ, Peng XH, Liu X, Zhang B, Xu X, Li XP (2018) Exosomal miR-9 inhibits angiogenesis by targeting MDK and regulating PDK/AKT pathway in nasopharyngeal carcinoma. *J Exp Clin Cancer Res* 37:147
- Ma Z, Wang Y, Piao T, Liu J (2016) Echinocystic acid inhibits IL-1beta-induced COX-2 and iNOS expression in human osteoarthritis chondrocytes. *Inflammation* 39:543–549
- Mansell JP, Tarlton JF, Bailey AJ (1997) Biochemical evidence for altered subchondral bone collagen metabolism in osteoarthritis of the hip. *Br J Rheumatol* 36:16–19
- Min Z, Zhang R, Yao J, Jiang C, Guo Y, Cong F, Wang W, Tian J, Zhong N, Sun J, Ma J, Lu S (2015) MicroRNAs associated with osteoarthritis differently expressed in bone matrix gelatin (BMG) rat model. *Int J Clin Exp Med* 8:1009–1017
- Nugent M (2016) MicroRNAs: exploring new horizons in osteoarthritis. *Osteoarthr Cartil* 24:573–580
- Patterson AM, Cartwright A, David G, Fitzgerald O, Bresnihan B, Ashton BA, Middleton J (2008) Differential expression of syndecans and glypicans in chronically inflamed synovium. *Ann Rheum Dis* 67:592–601
- Salminen-Mankonen H, Saamanen AM, Jalkanen M, Vuorio E, Pirila L (2005) Syndecan-1 expression is upregulated in degenerating articular cartilage in a transgenic mouse model for osteoarthritis. *Scand J Rheumatol* 34:469–474
- Shannon P, Markiel A, Ozier O, Baliga NS, Wang JT, Ramage D, Amin N, Schwikowski B, Ideker T (2003) Cytoscape: a software environment for integrated models of biomolecular interaction networks. *Genome Res* 13:2498–2504
- Shi B, Wang Y, Zhao R, Long X, Deng W, Wang Z (2018) Bone marrow mesenchymal stem cell-derived exosomal miR-21 protects C-kit+ cardiac stem cells from oxidative injury through the PTEN/PI3K/Akt axis. *PLoS One* 13:e0191616
- Shin YS, Yoon JR, Kim HS, Lee SH (2018) Intra-articular injection of bone marrow-derived mesenchymal stem cells leading to better clinical outcomes without difference in MRI outcomes from baseline in patients with knee osteoarthritis. *Knee Surg Relat Res* 30:206–214
- Smyth GK (2004) Linear models and empirical Bayes methods for assessing differential expression in microarray experiments. *Stat Appl Genet Mol Biol* 3:3
- Song J, Kim D, Chun CH, Jin EJ (2013) MicroRNA-9 regulates survival of chondroblasts and cartilage integrity by targeting protogenin. *Cell Commun Signal* 11:66
- Wen D, Peng Y, Liu D, Weizmann Y, Mahato RI (2016) Mesenchymal stem cell and derived exosome as small RNA carrier and immunomodulator to improve islet transplantation. *J Control Release* 238:166–175
- Xu JF, Yang GH, Pan XH, Zhang SJ, Zhao C, Qiu BS, Gu HF, Hong JF, Cao L, Chen Y, Xia B, Bi Q, Wang YP (2014) Altered microRNA expression profile in exosomes during osteogenic differentiation of human bone marrow-derived mesenchymal stem cells. *PLoS One* 9:e114627
- Yamaguchi R, Yamamoto T, Motomura G, Ikemura S, Iwasaki K, Zhao G, Doi T, Iwamoto Y (2014) Bone and cartilage metabolism markers in synovial fluid of the hip joint with secondary osteoarthritis. *Rheumatology (Oxford)* 53:2191–2195
- Zhang D, Lee H, Zhu Z, Minhas JK, Jin Y (2017) Enrichment of selective miRNAs in exosomes and delivery of exosomal miRNAs in vitro and in vivo. *Am J Physiol Lung Cell Mol Physiol* 312:L110–L121
- Zhang H, Song B, Pan Z (2018) Downregulation of microRNA-9 increases matrix metalloproteinase-13 expression levels and facilitates osteoarthritis onset. *Mol Med Rep* 17:3708–3714

Publisher's note Springer Nature remains neutral with regard to jurisdictional claims in published maps and institutional affiliations.